Functional polyketones for the removal of calcium and magnesium from water (Part II)

Figaroa, Patrick; Miedema, Henk; Euverink, Gerrit; Picchioni, Francesco

Published in:
Pure and Applied Chemistry

DOI:
10.1515/pac-2016-1007

Publication date:
2017

Conference paper

Patrick A. Figaroa*, Henk Miedema, Gert-Jan Euverink and Francesco Picchioni*

Functional polyketones for the removal of calcium and magnesium from water (Part II): cross-linking and functional characterization

DOI 10.1515/pac-2016-1007

Abstract: Functional polyketones were chemically cross-linked for the softening of hard water, i.e. for the removal of the divalent cations Ca^{2+} and Mg^{2+}. Elemental analysis, FT-IR spectroscopy, solubility- and swelling-experiments were used to demonstrate the occurrence of the cross-link reaction. Testing the different compounds for their Ca^{2+} and Mg^{2+} removal capacity assessed the structure-functionality of the polymers. The corresponding water-insoluble resins were then tested for their Ca^{2+} and Mg^{2+} removal capacity-performance being explained in terms of their chemical structure. Ion adsorption of these polymers is not based on an ion exchange, the prevailing mechanism for most currently existing adsorption resins. Rather, the amino functionalized polymers synthesized here adsorb cations as well as their accompanying anionic counterparts, possibly through a chelating mechanism. The obtained results show that functional polyketones are promising in this context as they are easily tunable with the chemical nature of the N-containing groups determining the affinity of the polymer for Ca^{2+} and/or Mg^{2+}.

Keywords: adsorption; cross-link; elemental analysis; FT-IR spectroscopy; hard water; inductively coupled plasma (ICP) mass spectrometry; ion chromatography; POC-16.

Introduction

Hard water, containing significant amounts of divalent calcium and magnesium cations, is a worldwide problem in domestic and industrial applications. The presence of these cations in water occurs naturally in countries where ground water is extracted from soil containing limestone, sedimentary rock or calcium/magnesium bearing minerals. According to wide-spread drinking water quality standards [1], the total amount of dissolved calcium and magnesium should lie below 75 ppm even though intake of hard water is not directly health threatening [2]. Hard water is the leading cause of scaling in water-using equipment, resulting in more energy consumption due to restricted water flow and reduced heat transfer capabilities. Furthermore, hard water increases the consumption of unnecessary over-dosed quantities of cleaning agents [3]. The harsh ionic conditions the equipment is exposed to, for example during cleaning protocols, reduces its lifetime. Specific technologies to treat hard water include adsorption (e.g. polyelectrolytes and zeolites), membrane systems

Article note: A collection of invited papers based on presentations at the 16th International Conference on Polymers and Organics Chemistry (POC-16), Hersonissos (near Heraklion), Crete, Greece, 13–16 June 2016.

***Corresponding authors: Patrick A. Figaroa and Francesco Picchioni,** Department of Chemical Engineering/Product Technology, ENTEG, University of Groningen, Nijenborgh 4, 9747 AG, Groningen, The Netherlands, e-mail: patrick.figaroa@wetsus.nl (P. A. Figaroa), f.picchioni@rug.nl (F. Picchioni)
Henk Miedema: Wetsus, European Center of Excellence for Sustainable Water Technology, Oostergoweg 9, 8911 MA, Leeuwarden, The Netherlands
Gert-Jan Euverink: Products and Processes for Biotechnology, ENTEG, University of Groningen, Groningen, The Netherlands

(e.g. nanofilters/ultrafilters or electrodialysis), chemical precipitation-coagulation, micellar-enhanced ultrafiltration, biomaterials, magnetic treatment and scale inhibitors [1, 4–14]. However, despite the capabilities of such technologies to treat hard water, they posses disadvantages and limitations that hinder their applicability in practical situations [15, 16].

Recently, functional polyketones (e.g. polyketones containing amines and its derivatives) able to extract Ca^{2+} and Mg^{2+} from water were synthesized and characterized [17]. These materials were cross-linked with 1,6-hexamethylendiamine, and subsequently explored for their adsorption removal capabilities in synthetic solutions resembling hard water. The ability to remove Ca^{2+} and Mg^{2+}, as studied in batch experiments, was aimed to correlate with the amino functional groups present in the particular cross-linked polyketone. Cross-linking was performed here, in order to provide mechanical strength to the polymer and water thermal-insolubility, rigidity, high internal surface area and salt-accessibility to the internal functional binding sites. The objective in this study is to cross-link chemically modified polyketones and examine their calcium and magnesium (batch-mode, lab-scale) adsorption in relation to the molecular structure. Finally, the Ca^{2+} and Mg^{2+} adsorption-capacities were compared to discuss the chemical structure-function relationship of the synthesized cross-linked functional polyketones.

Experimental

Materials

1,6-Hexamethylendiamine (HDA, 98 %, from Sigma-Aldrich), methanol anhydrous, (MeOH, 99.8 %, from VWR), calcium chloride dihydrate ($CaCl_2.2H_2O$, > 99.0 %, from Sigma-Aldrich) and magnesium chloride hexahydrate ($MgCl_2.6H_2O$ > 99.0 %, from Sigma-Aldrich) were obtained and used without further purification. Functional polyketones with about 50 % pyrrole-units bearing amino functional side-chains along the backbone were prepared according to our previous work [17]. $CaCl_2.2H_2O$ and $MgCl_2.6H_2O$ solutions were dissolved in Milli-Q water.

Cross-linking reactions

The functional polyketones according to our previous work [17] were immediately cross-linked with HDA after functionalization (see Fig. 1) in the presence of MeOH in a 100 mL round bottom glass reactor with oval stirrer, and under oil bath-controlled temperature conditions. The weight ratio functional polyketones: HDA applied varied between 0.100 and 0.120 based on weights of functional polyketone < 30 g (see Appendix). Each functional polyketone was first dissolved in ca. 20 mL MeOH at 60 °C. HDA was then dissolved in ca. 10 mL MeOH and added drop-wise to 10 g of functional polyketone in 10 min time, at a stirring speed of around 1100 rpm. The temperature was then slowly raised to 120–130 °C in order to allow MeOH and the by-product water to evaporate. The reaction time varied from 10 to 20 min, depending on the material and the moment stirring became too hampered due to the high viscosity of the reaction mixture.

The completion of the reaction leading to the cross-linked functional polyketones was visually, clearly notable from the abrupt color change, from light to dark-brown, reflecting the transition from the viscous rubbery paste into the solid end-product. Prior to a solubility test in MeOH at a concentration of approximately 125 mg/L, the material was recovered with liquid N_2 from the reactor after cooling down to room temperature, grinded into small particles, washed multiple times with an excess of Milli-Q water and dried in a vacuum oven evaporator at 100 mbar and 40 °C overnight. As demonstrated by the solubility test, in contrast to the non-cross-linked functional polyketones, cross-linked ones did not dissolve in MeOH indicating a successful reaction between the functional polyketones and HDA. The cross-linked network plays a crucial role in the mechanical strength of the polymer network. This facilitates a solid product formulation with higher capacities than the liquid type of sorbents and thus lowers, for example, construction and handling costs.

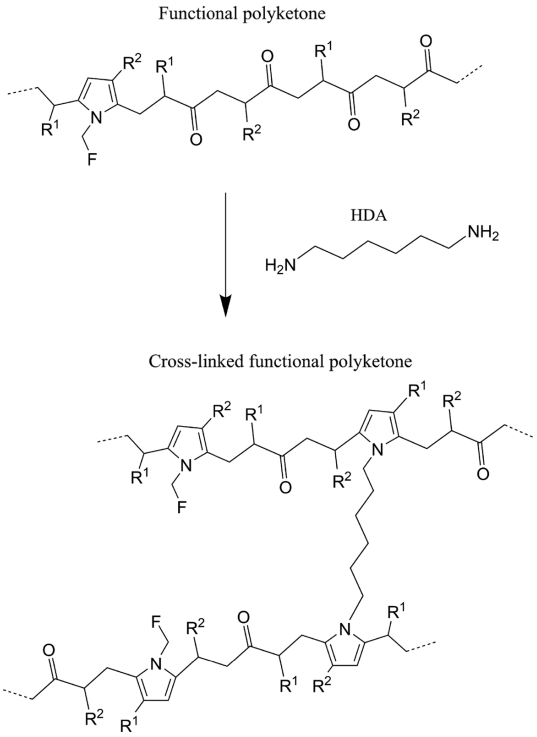

Fig. 1: Irreversible cross-link reaction scheme for functional polyketones. Functional-, unreacted- and cross-linked monomeric-units are depicted in the prepared molecular structure (below). F represents the type of pending functionality.

Characterization techniques

Elemental analyses (EA)

The increase of nitrogen content after the cross-link reactions was obtained by elemental analyses (Table 1), suggesting a successful reaction between the functional polyketones and HDA. Elemental analysis of nitrogen in wt. % was performed with a Euro EA elemental analyzer in duplo by using approximately 2 mg of each dry prepared functional polyketone.

Table 1: Values of nitrogen content after cross-linking the functional polyketones.

Functional polyketone (name)	N_e^{CL} (g/g)
PK30-BA	0.069
PK30-API	0.124
PK30-AEP	0.112
PK30-2DME	0.093
PK30-1,3DAP	0.099
PK30-DEE	0.097
PK30-1,2DAP	0.105
PK30-4PcA	0.101

Fourier transform infrared spectroscopy (FT-IR, KBr)

Spectra were recorded with a Perkin Elmer Spectrum 2000 or an IR tracer – 100 Shimadzu by using approximately 5 mg of cross-linked solid product and 5 mg of functional polyketone solubilized in 5 mL MeOH. The decrease in intensity of the vibrational band on the ketone oxygen C=O reacted site for cross-linking relative

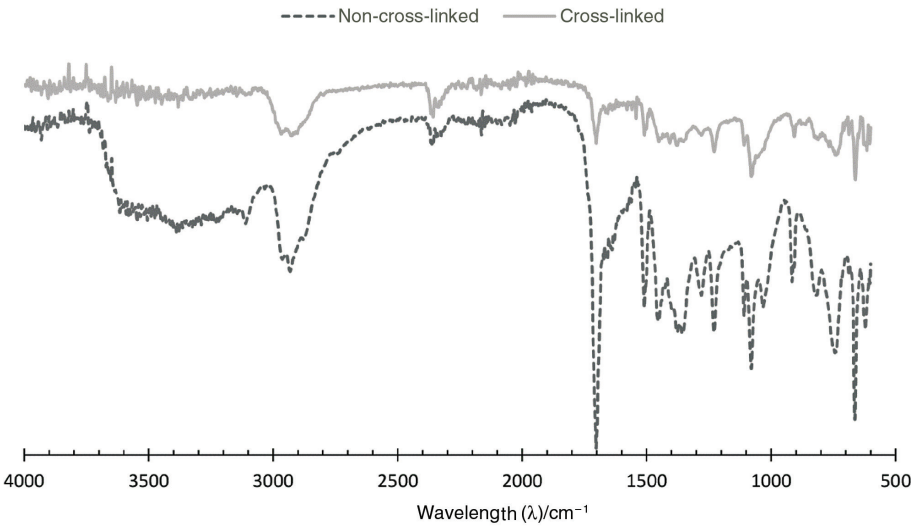

Fig. 2: FT-IR spectra before (lower spectrum) and after (upper spectrum) the cross-link reaction of PK30-API with HDA. Note the decrease in intensity of the peak at 1700 cm^{-1} and increase in intensity of the peak at 1050 cm^{-1} from the lower- to the upper-spectrum. This relative change represents conversion from C=O units to pyrrole units C_4H_2N (30 %) or C_5H_4N (70 %).

to the increase in intensity of the reacted pyrrole ring breathing 1050 cm^{-1} on the polymer backbone, was identified at 1700 cm^{-1} and establishes a successful reaction between the functional polyketones and HDA, see Fig. 2 for this example.

Swelling degree

The swelling degree (% SD) indicates and provides insights into the existence and extent of molecular inter-chain interactions. Swelling creates a higher internal surface area, thereby increasing the accessibility of the polymer functional binding sites [18, 19]. The % SD depends on the wet mass (m_{wet}) and dry mass (m_{dry}) of the polymer and is defined as:

$$\% \text{ SD} = \frac{m_{wet} - m_{dry}}{m_{dry}} \cdot 100 \quad (1)$$

In general, a relatively high % SD indicates a low cross-link density and *vice versa*. The % SD was measured by immersing approximately 0.30 g of dry grinded cross-linked functional polyketone with particle diameter varying between 50 and 500 μm in 20 mL Milli-Q water for 1, 4, 15, and 36 h. The wet cross-linked functional polyketones were collected at each time point by vacuum filtration and weighted to determine their water-uptake. Values of % SD as average were taken in order to interpret the relation between the % SD and the N-groups. The swell-ability is an indirect, qualitatively and independent measure for the degree of the cross-linking reactions.

Batch experiments

Adsorption-capacities were studied in batch mode with different types of amino functionalities including aliphatic and aromatic-like structures at initial molar ratios of divalent cation: N-groups on the cross-linked functional polyketones (including those of the pyrrole group on the backbone) of about 0.3 for Ca^{2+} and 0.1 for Mg^{2+}. These experiments were performed in a 250 mL round bottom flask with oval magnetic stirrer for 40 min. In general, 0.75 g of dry grinded cross-linked functional polyketones were added to 100 mL (solu-

tion of salt with Milli-Q) of the 0.3 Ca^{2+}: N-groups and 0.1 Mg^{2+}: N-groups containing solutions. The low salt concentrations allow a proper comparison of the adsorption performance between each functional group avoiding an oversaturation condition of Ca^{2+} or Mg^{2+}. After an exposure time of 40 min to the cationic solutions, the filtrate was collected with a vacuum glass filter with a pore size range 1–16 μm. To compensate for loss of solution due to filtration and swelling, the filtrate was filled up to its initial volume of 100 mL with Milli-Q water. Cation concentrations were measured by conductometry and interactions were determined as the decline of cation concentration in the salt solution. Adsorption-capacities were defined as the molar ratio of bound divalent cation and N-groups on the cross-linked functional polyketone i.e. [mmol cation-bounded] : [mmol N-groups].

Ion concentration measurements

Ca^{2+} concentrations were measured by ICP (inductively coupled plasma) using a Perking Elmer 53 000 DV and Cl^- concentrations with IC (ion chromatography) using a Metrohm IC Compact 761. Samples were filtered with a hydrophilic PTFE 0.45 μm syringe-filter and measured at a dilution factor of 1001 in Milli-Q water.

Results and discussion

Relation between N-groups and swelling degree

In order to estimate the degree or cross-link density (defined here as the number of HDA reacted per di-carbonyl groups, Fig. 1), the nitrogen percentage increase (% NPI) was calculated by using the nitrogen content as determined by elemental analysis, before ($N_e^{0.5}$) and after (N_e^{CL}) the cross-link reaction (see Table 1). % NPI was defined as follows: $N_e^{CL} \times 100 / N_e^{0.5} - 100$. Note in Table 1 that the increase in nitrogen does not surpass the maximum allowed HDA to react for all functional polyketones (see Appendix) even if an excess HDA was used. This is because the high concentrations increase the reactivity at a higher rate [19]. Since the unreacted amines remained in the mixture, at lower or even equal concentrations to the N-groups, the reaction becomes kinetically inhibited. In general, when the cross-link density is low (and thus the % NPI), the swelling degree (% SD) is expected to be high and *vice versa*.

The relation between % NPI and % SD for all the cross-linked functional polyketones tested is displayed in Fig. 3, showing the correlation between the two parameters. Despite the scattering of the data points in the range of 0–25 % SD, the plot shows a tendency of increasing % SD with decreasing % NPI with the only, yet unexplained, exception of 1,2DAP. It seems that this functional group interacts better with water compared to 4PcA, 2DME and API bearing all a relatively lower % NPI. The reason is most probably due to the shorter distance of the nitrogen atom from the side-chain to the nitrogen atom at the pyrrole group, by that increasing its polarity. The plot also shows an additional outlier, i.e. PK30-BA. The relatively high % NPI for PK30-BA can be understood by assuming a reaction mechanism involving imine bond formation, requiring twice as much HDA leading to a relatively higher nitrogen content.

The observed variation in % NPI may be understood by the difference in cross-link reaction kinetics due to the solubility of the functional polyketones in MeOH, with the ones with higher solubility giving rise to faster kinetics. The reaction kinetics differed per functional polyketone and thus completion of the cross-link reaction may have not taken place in some cases due to the sudden change in composition. Since the % SD strongly depends on the polarity, the cross-link density, the molecular structure, the reaction conditions and the reaction kinetics, it is yet difficult to create cross-link functional polyketones with similar swell-ability and thus similar porosity.

Confirmation of the hypothesis mentioned above, a high % SD correlates with a low % NPI, requires to investigate the relation between the two parameters with one cross-linked functional polyketone. The effect of % NPI on % SD could be studied by varying the time of cross-linking, which, in turn, affects the cross-link

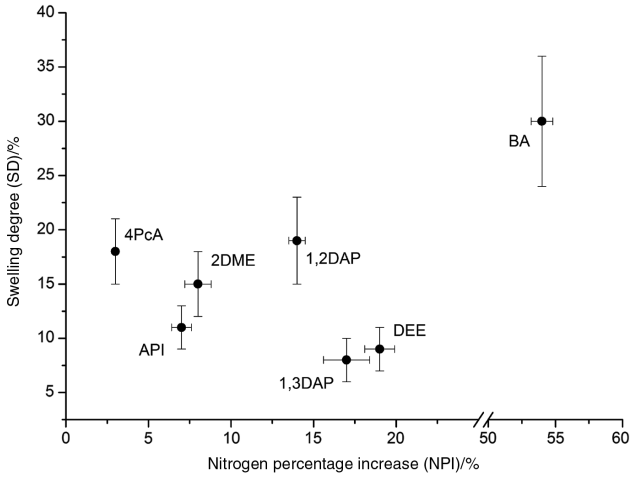

Fig. 3: Swelling degree as function of the nitrogen content of the functional polyketones relative to the nitrogen content after cross-linking. The abbreviations shown in the figure indicate the functional groups attached as pending groups on the cross-linked functional polyketone. Error bars indicate standard deviations.

density, and by that the % NPI. Nevertheless, apart from the observed scattering of the data in Fig. 3, the value of % NPI does give an indication of the swell-ability of the particular cross-linked functional polyketone.

Molecular structure affects calcium and magnesium adsorption-capacity

The broader scope of the current study was to cross-link functional polyketones that can be used to soften hard water, i.e. remove divalent cations, notably Ca^{2+} and Mg^{2+}. These cross-linked functional polyketones, including aliphatic and aromatic architectures, were synthesized with the main idea to find a molecular structure selective for Ca^{2+} and/or Mg^{2+}. Therefore, preliminary adsorption tests were performed. Figure 4 summarizes for all cross-linked functional polyketones, the Ca^{2+} (dark bars) and Mg^{2+} (light bars) specific adsorption-capacity, defined as the molar ratio of the adsorbed cation and N-groups on the particular cross-linked functional polyketones. The molar ratio cation-bounded: N-groups is expressed as function of the swelling degree (% SD) during an hour of water uptake. The molar ratio between the divalent cation present in solution and the N-groups of the cross-linked functional polyketone (including those belonging to the pyrrole groups along the polymer backbone) was around 0.3 and 0.1 for Ca^{2+} and Mg^{2+}, respectively. It is expected that the % SD affects the adsorption-capacity and/or kinetics due to its effect on the accessibility of the polymer for Ca^{2+}/Mg^{2+} (and chloride Cl^{-}, later on discussed in detail). Apart from % SD it is expected that the identity of the N-groups is a defining parameter in the adsorption of Ca^{2+} and Mg^{2+} as well. Because PK30-API demonstrated the highest specificity, i.e. largest difference between Ca^{2+} and Mg^{2+} adsorption (Fig. 4), FT-IR was applied to PK30-API in the presence of either Ca^{2+} and Mg^{2+} denoted in the figure as Ca and Mg. The results are depicted in Fig. 5. The specific absorption peaks of PK30-API appeared at 1700 cm^{-1} (C=O stretch) and 1455 cm^{-1} (C=C pyrrole stretch). This result is in agreement with a previous study [20]. The appearance of the peak at 3300 cm^{-1} and 1000 cm^{-1} is attributed to the influence of the salt concentration, both for Ca^{2+} and Mg^{2+} while the peak positioned at 2800 cm^{-1} is assigned to the solvent MeOH. As can be seen from Fig. 5, the intensity at 1700 cm^{-1} and 1455 cm^{-1} decreased after treatment with Ca^{2+} but remained unaffected by Mg^{2+} indicating that Ca^{2+} interacts with the carbonyl groups and the pyrrole ring. The corresponding model compound spectra showed a similar decrease in adsorption band around 1450 cm^{-1} after treatment with both Ca^{2+} and Mg^{2+} with the vibrational band of Mg^{2+} being more intense after treatment, but for brevity this model compound spectra was not given.

Since the vibrational bands of the pending imidazole groups could not be seen because of the overlapping peaks in the region of the band of MeOH, one could not establish a direct interaction with its pending

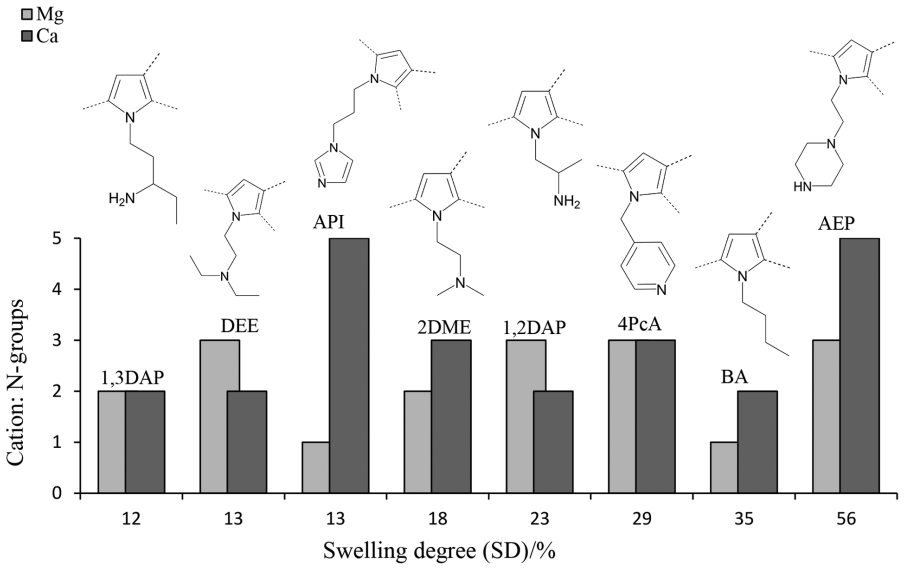

Fig. 4: Adsorption-capacities of Ca^{2+} (dark bars) and Mg^{2+} (light bars) as a function of the % SD during 1 h of water uptake. These studies were performed at initial molar ratios divalent cation: N-groups on the cross-linked functional polyketone of about 0.3 for Ca^{2+} and 0.1 for Mg^{2+}. The molar ratio cation-bounded: N-groups is denoted in the figure at the y-axis as cation: N-groups (e.g. percentage). The abbreviations for the type of functional groups attached as a side chain to the polymer and their corresponding molecular structures after functionalization are given in the figure. For brevity, R-, unreacted- and cross-linked monomeric-units are not shown.

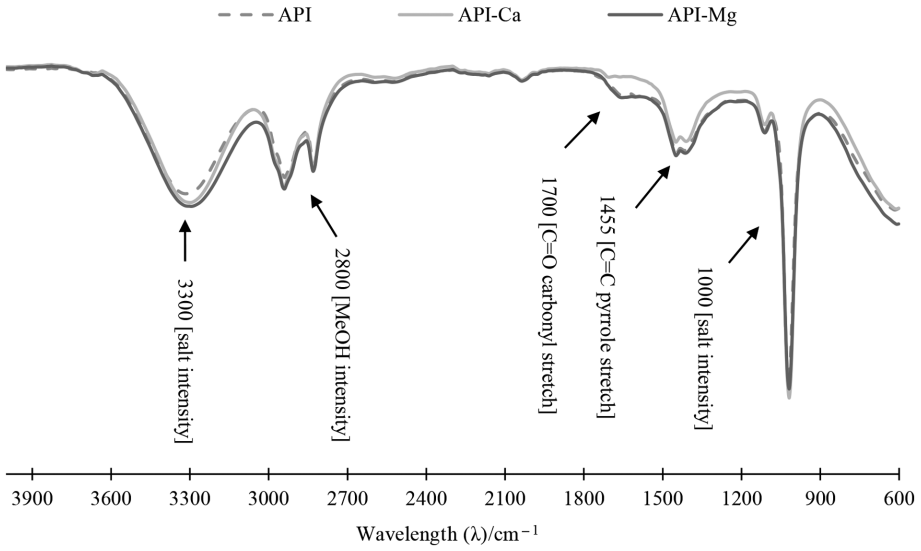

Fig. 5: FT-IR spectra of PK30-API before (API) and after treatment with Ca^{2+} (API-Ca) and Mg^{2+} (API-Mg) for 7 days mixing at room temperature of initial molar ratios divalent cation: N-groups of about 0.3 for Ca^{2+} and 0.1 for Mg^{2+}.

functionality through FT-IR measurements. However, as can be seen from Fig. 5, the intensity at 1700 cm^{-1} and 1455 cm^{-1} decreased after treatment with Ca^{2+} but remained unaffected by Mg^{2+} indicating that Ca^{2+} interacts with the carbonyl groups and the pyrrole ring. This result indicates non-specific and structure-dependent binding of Ca^{2+} over Mg^{2+}. Even though unnoticed in Fig. 5, interaction between the pending imidazole group and Ca^{2+} accounts for the substantial higher Ca^{2+} adsorption of PK30-API as observed in Fig. 4. In conclusion, rather than the identical backbone, the pending functional groups of the modified PK30 compounds studied here determine to a large extent the specificity between Ca^{2+} and Mg^{2+} adsorption.

As remarked before, unfortunately it is hard, if not impossible, to design and synthesize different chemically modified polyketones all demonstrating equal % SD. Consequently, Fig. 4 shows the Ca^{2+} and Mg^{2+} adsorption in relation to both pending functionality and % SD. For now, the isolated effect of either parameter cannot be delineated. But whatever the contribution of either parameter is on the measured cation adsorption, Fig. 4 allows drawing some conclusions already. First, swelling does not dominate the cation adsorption-capacity. Actually, as obvious from Fig. 4 the adsorption-capacity is rather insensitive to the swelling degree. In second place, even though non-specific adsorption contributes to the total adsorption-capacity, the mechanism of adsorption is certainly not entirely non-specific, some compounds show higher affinity for Ca^{2+}, others for Mg^{2+}. For example, even though PK30-API and PK30-DEE both show an % SD of 13, PK30-API demonstrates the highest Ca^{2+} adsorption-capacity and PK30-DEE the highest Mg^{2+} adsorption-capacity. A second example comes from the Mg^{2+} and Ca^{2+} adsorption-capacity of PK30-AEP. Note that the Ca^{2+} adsorption-capacity of PK30-AEP is similar to that of PK30-API whereas its Mg^{2+} adsorption-capacity is similar to that of PK30-DEE, even though their % SD differ significantly, 56 for PK30-AEP and 13 for both PK30-API and PK30-DEE. In contrast to the % SD, the number and identity of the N-groups added to the side chain affects the adsorption-capacity. If the individual Ca^{2+} and Mg^{2+} adsorption-capacities of each cross-linked functional polyketone were added, the control PK30-BA (lacking N-groups in the pending side chain) would contribute to a low adsorption-capacity. However, we interpret this finding as evidence that functionalization as side chains with amino groups improves the divalent cation adsorption-capacity. Given the difference in electronegativity of, for instance, a primary, secondary and tertiary nitrogen, it comes to no surprise that the chemical structure determines, at least to some extent, cation adsorption, in terms of capacity as well as in specificity. For example, the spacer of three carbon atoms and the aromatic functional group as side branch in PK30-API determines the affinity of Ca^{2+} over Mg^{2+} while the spacer of two carbon atoms and a linear (semi-dendrimer) type in PK30-DEE the affinity of Mg^{2+} over Ca^{2+}. In addition, differences between Ca^{2+} and Mg^{2+} chemistry may contribute as well. Most likely, Fig. 4 reflects the combined effects of N-groups and cation species on the observed adsorption behavior of the different compounds studied.

It should be noted that the Ca^{2+} and Mg^{2+} adsorption removal ability displayed by the cross-linked functional polyketones presented here is not based on an ion exchange mechanism. In contrast, the working mechanism of most currently existing adsorption resins is based on ion exchange. Once saturated, these ion exchange resins need to be regenerated. Common procedure holds to use a rather acidic or caustic solution and substitute the Ca^{2+} bound to the resin by either H^+ or Na^+. By implication, H^+ or Na^+ is released as soon as the resin is re-used for Ca^{2+} adsorption. This H^+ or Na^+-containing effluent is commonly discharged into the environment. To avoid the use of H^+ or Na^+ all together, an adsorbent can be employed that takes up Ca^{2+} as well an accompanying anion, in this particular case Cl^-, at least given that the adsorbed $CaCl_2$ can be removed by washing out with demineralized water. The polyketones described in this study fulfill this condition. In an adsorption experiment with PK30-BA at a divalent cation: N-groups ratio of one, the measured Ca^{2+} and Cl^- uptake was 0.0211 and 0.0394 mol, respectively. Given the 6 % error of ICP and IC, this finding corresponds to the expected molar ratio for $CaCl_2$ adsorption. Experiments including PK30-API gave similar molar Ca^{2+}/Cl^- adsorption ratios. The adsorption of both Ca^{2+} and Cl^- is a key advantage of the type of chemistry employed here as it avoids an acidic or caustic waste stream due to the otherwise necessary regeneration of the resin.

Fine tuning the chemistry and improving the structure – function relationship is the focus of future study. Two other aspects that need to be paid attention to in future research is the behavior of these modified polyketones under continuous flow conditions and the ability to regenerate them by temperature. Both are key aspects from the technological application point of view, as well as in the context of economics.

Outlook for regeneration by temperature

Cation adsorption by the cross-linked functional polyketones presented here is based on an entirely different mechanism. Not only the cation is adsorbed but the accompanying anion, in this study Cl^-, as well. This feature circumvents the regeneration step typically applied for ion exchange resins, thereby avoiding a H^+ or

Na^+-loaded effluent waste stream. Obviously, the cross-linked functional polyketone needs to be regenerated as well once they are saturated with Ca^{2+} and/or Mg^{2+} and the accompanying anion Cl^-. Washing out with demineralized water is one option. Current research includes exploring the temperature sensitivity of the ion adsorption-desorption process of the different polymers. If successful, the chemical regeneration step can be replaced by a temperature step.

Conclusions

This study confirms the versatility of the cross-linked functional polyketones derived by Paal–Knorr modifications in the preparation of adsorbents with tailored complexation abilities towards soluble chloride salts of calcium and magnesium. Preliminary adsorption experiments are promising in the context of specificity, i.e. the chemical structure of the N-groups determines to some extent the affinity of the polymer for calcium and/or magnesium. The cross-linked functionalized polyketones reported here co-adsorb the accompanying anion as well and do not exchange divalent ions with monovalent ions. This implies that the purified water has a lower total dissolved salt content. The potential possibility of thermal regeneration instead of chemical regeneration generates less waste material with a lower salt content, thereby improving the sustainability of the process.

Acknowledgments: This work was performed in the cooperation framework of Wetsus, European Centre of Excellence for Sustainable Water Technology (www.wetsus.nl). Wetsus is co-funded by the Dutch Ministry of Economic Affairs and Ministry of Infrastructure and Environment, the European Union Regional Development Fund, the Province of Fryslân, and the Northern Netherlands Provinces. The authors like to thank the participants of the research theme Desalination for the fruitful discussions and their financial support. This work is part of the research program of University Campus Fryslân (UCF) (Grant/Award Number: S010.01), which is financed by the Province of Fryslân.

Appendix

Calculations for the synthesis of the cross-linked functional polyketones

The amount of HDA require to obtain a solid composition of particles was higher than the amount calculated. The reason why the calculation underestimates the actual amount required is most likely related to the kinetic effects [19]. However, it is believed here that solid particles after cooling could be obtained by using the exact amount of HDA by increasing the reaction time via extrusion. The synthesis of the cross-linked functional polyketones described here involves the reaction of functional polyketone PK30-DEE (212 g/mol) as an example, with HDA (MW, 116.21). In order to optimize the process conditions, amount of HDA is estimated, given the reaction mechanism. The amount required to cross-link two PK30-DEE chains, with a carbonyl conversion of 50 %, by similar 1,4-dicarbonyl (pyrrole) unit formation is as follows:

Starting from 100 g of PK30 (MW = 131.6 g/mol), the number of 1,4-dicarbonyl units is $(100/131.6) \times 0.50 = 0.380$ mol, implying $0.380 \times 2 = 0.760$ mol of un-reacted, free single carbonyl units (MW = 131.6/2 = 65.8 g/mol) and $(100/131.6) \times 0.50 = 0.380$ mol of reacted carbonyl units. The end weight of PK30-DEE is thus $(0.760 \times 65.8) + (0.380 \times 212) = 131$ g. The molar 1,4-dicarbonyl fraction possible for cross-link is $[(0.67 - 0.50)/0.67] = 0.254$ while the remaining free containing number of 1,4-dicarbonyl mol available for cross-link is 0.380. Since only the fraction of 0.254 is allowed to react, the practical number of 1,4-dicarbonyl mol/g of PK30-DEE is $(0.254 \times 0.380)/131 = 0.000738$. By taking 10 g of PK30-DEE, the number of HDA needed to connect two polymeric chains is then $(0.000738 \times 10 \times 116.21)/2 = 0.429$ g.

References

[1] B. Van der Bruggen, H. Goosen, P. A. Everard, K. Stemgee, W. Rogge. *J. Environ. Manag*. **91**, 541 (2009).
[2] J. K. Fawell, U. Lund, B. Mintz. *Guidelines for drinking water quality*, **2,** 1 (1996).
[3] N. Ferlin, D. Grassi, C. Ojeda, M. J. L. Castro, A. Fernandez-Cirelli, J. Kovensky, E. Grand. *J. Surfact. Deterg*. **15**, 259 (2012).
[4] M. M. Saleh. *Desalination* **235**, 319 (2009).
[5] I. Arrigo, P. Catalfamo, L. Cavallari, S. Di Pasquale. *J. Hazard Mater.* **147**, 513 (2007).
[6] M. E. Mahmoud, A. A. Yakout, H. Abdel-Aal, M. M. Osman. *Bioresour. Technol.* **134**, 324 (2013).
[7] S. B. Shadizeh, R. W. Taylor, J. F. Scamehorn, A. L. Schovanec, S. D. Christian. *Metal-Ion Separation and Preconcentration* **716**, 280 (1990).
[8] C. Qin, R. Wang, W. Ma. *Chem. Eng. J.* **156**, 540 (2010).
[9] N. Kabay, M. Demircioglu, E. Ersöz, I. Kurucaovali. *Desalination* **149**, 343 (2002).
[10] B. Mahmoud, M. Yosra, A. Nadia. *Sep. Purif. Technol.* **171**, 88 (2016).
[11] Z. Amjad, P. G. Koutsoukos. *Desalination* **335**, 55 (2014).
[12] A. A. Al-Hamzah, C. M. Fellows. *Desalination* **359**, 22 (2015).
[13] M. A. Migahed, S. M. Rashwan, M. M. Kamel, R. E. Habib. *J. Mol. Liquids* **224**, 849 (2016).
[14] K. D. Demadis. *Desalination Res. Prog.* Chapter VI, **1**, 1249 (2008).
[15] S. Seo, H. Jeon, J. K. Lee, G. Kim, D. Park, H. Nojima, J. Lee, S. Moon. *Water Res.* **44**, 2267 (2010).
[16] S. S. Cob, C. Beaupin, B. Hofs, M. M. Nederlof, D. J. H. Harmsen, E. R. Cornelissen, A. Zwijnenburg, F. E. G. Guner, G. J. Witkamp. *Desalination Water Treat.* **51**, 936 (2013).
[17] P. A. Figaroa, H. Miedema, G. J. W. Euverink, F. Picchioni. *16th International Conference Polymers and Organic Chemistry*. Part I, (2016).
[18] S. Nomanbhay, K. Palanisamy. *Electron. J. Biotechnol.* **8**, 43 (2005).
[19] L. Hua, H. N. Hou. *Electronic Packaging Technology & High Density Packaging*. 1 (2008).
[20] C. Toncelli, A. Haijer, F. Alberts, A. A. Broekhuis, F. Picchioni. *Ind. Eng. Chem. Res*. **54**, 9450 (2015).